

Cathodoluminescence of high-pressure feldspar minerals as a shock barometer

Masahiro KAYAMA ^{1,2,*}, Toshimori SEKINE^{3,4}, Naotaka TOMIOKA ⁵, Hirotugu NISHIDO⁶, Yukako KATO³, Kiyotaka NINAGAWA⁷, Takamichi KOBAYASHI⁸, and Akira YAMAGUCHI ^{9,10}

¹Department of Earth and Planetary Materials Science, Graduate School of Science, Tohoku University, Sendai 980-8578, Japan

²Creative Interdisciplinary Research Division, Frontier Research Institute for Interdisciplinary Sciences, Tohoku University, Sendai 980-8578, Japan

³Department of Earth and Planetary Systems Science, Graduate School of Science, Hiroshima University, Higashi-Hiroshima 739-8526, Japan

⁴Center for High Pressure Science and Technology Advanced Research, Pudong, Shanghai 201203, China

⁵Kochi Institute for Core Sample Research, Japan Agency for Marine-Earth Science and Technology, 200 Monobe Otsu, Nankoku City, Kochi 783-8502, Japan

⁶Department of Biosphere-Geosphere Science, Okayama University of Science, 1-1 Ridaicho, Kita-ku, Okayama 700-0005, Japan

⁷Department of Applied Physics, Okayama University of Science, 1-1 Ridaicho, Kita-ku, Okayama 700-0005, Japan

⁸National Institute for Materials Science, 1-1 Namiki, Tsukuba, Ibaraki 305-0044, Japan

⁹National Institute of Polar Research, Tachikawa, Tokyo 190-8518, Japan

¹⁰Department of Polar Science, School of Multidisciplinary Science, SOKENDAI (The Graduate University for Advanced Studies), Hayama, Tokyo 190-8518, Japan

*Corresponding author. E-mail: masahiro.kayama.a3@tohoku.ac.jp

HPSTAR
597-2018

(Received 29 August 2017; revision accepted 11 March 2018)

Abstract—Cathodoluminescence (CL) analyses were carried out on maskelynite and lingunite in L6 chondrites of Tenham and Yamato-790729. Under CL microscopy, bright blue emission was observed in Na-lingunite in the shock veins. Dull blue-emitting maskelynite is adjacent to the shock veins, and aqua blue luminescent plagioclase lies farther away. CL spectroscopy of the Na-lingunite showed emission bands centered at ~330, 360–380, and ~590 nm. CL spectra of maskelynite consisted of emission bands at ~330 and ~380 nm. Only an emission band at 420 nm was recognized in crystalline plagioclase. Deconvolution of CL spectra from maskelynite successfully separated the UV–blue emission bands into Gaussian components at 3.88, 3.26, and 2.95 eV. For comparison, we prepared K-lingunite and experimentally shock-recovered feldspars at the known shock pressures of 11.1–41.2 GPa to measure CL spectra. Synthetic K-lingunite has similar UV–blue and characteristic yellow bands at ~550, ~660, ~720, ~750, and ~770 nm. The UV–blue emissions of shock-recovered feldspars and the diaplectic feldspar glasses show a good correlation between intensity and shock pressure after deconvolution. They may be assigned to pressure-induced defects in Si and Al octahedra and tetrahedra. The components at 3.88 and 3.26 eV were detectable in the lingunite, both of which may be caused by the defects in Si and Al octahedra, the same as maskelynite. CL of maskelynite and lingunite may be applicable to estimate shock pressure for feldspar-bearing meteorites, impactites, and samples returned by spacecraft mission, although we need to develop more as a reliable shock barometer.

INTRODUCTION

High-pressure Na and K-rich feldspars of lingunite and high-density plagioclase glass (maskelynite) formed due to a natural impact event are constituents of heavily

shocked stony meteorites and impactites (Mori 1990; Stöfler et al. 1991; Chen and El Goresy 2000; Tomioka et al. 2000; Jaret et al. 2015; Kato et al. 2017). Lingunite with a hollandite structure has been found in several L chondrites, H chondrites, and Martian

meteorites (El Goresy et al. 2000; Gillet et al. 2000; Tomioka et al. 2000; Liu 2006; Kato et al. 2017). As K-lingunite is stable at pressure from ~ 9 to ~ 26 GPa (Ringwood et al. 1967; Kinomura et al. 1975; Urakawa et al. 1994; Yagi et al. 1994; Tutti et al. 2001; Sueda et al. 2004; Liu 2006), the existence of lingunite in them provides firm evidence for high-pressure events that the parent bodies experienced. Maskelynite occurs widely in various types of shocked meteorite (e.g., lunar meteorites, shergottites, and ordinary chondrites) and impactites, and the occurrence constrains shock conditions in collision. Shock pressures for feldspar-bearing meteorites and impactites have been determined based on the paragenetic assemblage of maskelynite and high-pressure phases such as lingunite (Ostertag et al. 1986; Stöffler et al. 1986, 1991; El Goresy et al. 2000; Kubo et al. 2010). The refractive index measurement on the feldspar and maskelynite allows us to evaluate shock pressure in a range from ~ 15 to 45 GPa, although it requires their extraction in large amounts as a bulk analysis (Lambert 1981). Raman spectroscopy enables us to estimate shock pressure for a single maskelynite grain with a few micrometers size (Fritz et al. 2005). Cathodoluminescence (CL) spectroscopy of alkali feldspar and its shock-induced high-density glass has been proposed as a shock barometer with high spatial resolution ($\sim 1 \mu\text{m}$) over a wide pressure range (Kayama et al. 2012), but the calibration remains uncertain with regard to variations in shock temperature, duration time, and chemical compositions (Kayama et al. 2012).

CL is the emission of photons of ultraviolet (UV) to infrared (IR) wavelengths from a material stimulated by an incident electron beam, occurring by an excited level to ground state transition of electrons in specific lattice defect (e.g., oxygen deficiency and non-bridge oxygen hole center) or impurity (e.g., Ti^{4+} , Mn^{2+} , and Fe^{3+}) (Marfunin 1979; Marshall 1988; Yacobi and Holt 1990; Finch and Klein 1999; Götze et al. 1999, 2000). Therefore, CL microscopy and spectroscopy are powerful techniques for detection of lattice defects and trace elements and analysis of their distribution at detection limit of 0.1 ppm and spatial resolution of a few micrometers (Marshall 1988; Yacobi and Holt 1990; Götze et al. 1999, 2000). This method is very unique to investigate shock-induced defects in minerals (Kayama et al. 2012; Pittarello et al. 2015; Hamers et al. 2016).

CL analysis of minerals in meteorites and impactites has been used as an important tool for the clarification in shock metamorphism. Sipple and Spencer (1970) revealed a significant difference of CL spectral patterns of plagioclase between the Earth minerals and the Apollo breccias. The results indicate that a trace of impact event on the Moon remains in the lunar

samples. According to Owen and Anders (1980), CL imaging of quartz in the Cretaceous–Paleogene boundary, southeastern Colorado, differs in color-center variation from that in the volcanic ejecta, supporting the hypothesis that an impact event occurred at the end of the Cretaceous period. Furthermore, CL microscopy for shocked minerals has been extensively used to observe planar deformation features in quartz and feldspar (Boggs et al. 2001; Kayama et al. 2009; Hamers and Drury 2011) and visualize internal textures of moldavites (Fritzke et al. 2017). Since CL intensity and peak wavelength change with the degree of shock intense, CL spectroscopy of feldspar and quartz allows us to identify high-pressure silica phases (Chennaoui Aoudjehane et al. 2005) and to interpret impact histories based on the feldspar and quartz (Kayama et al. 2012; Pittarello et al. 2015; Hamers et al. 2016).

CL spectroscopy, with high spatial resolution ($\sim 1 \mu\text{m}$), of alkali feldspars and its shock-induced high-density glass has been developed to estimate shock pressure in meteorites and impactites, because CL peak intensity for samples experimentally shocked at known shock pressures increases linearly with increasing shock pressure (Kayama et al. 2012). Furthermore, the CL features such as intensity and peak wavelength are thought to depend on shock pressure that meteorites experienced and shock experiments imparted, rather than in-shock and postshock temperatures during these impact (Kayama et al. 2012). However, no CL investigations of shock metamorphism on plagioclase, maskelynite, and lingunite have been performed to date, in spite of feldspar with the Na-Ca composition being more abundant in chondritic meteorites and impactites than those with the K-Na composition.

Here, we extend to investigate CL properties of plagioclase, maskelynite, and lingunite in the L6 chondrites of Tenham and Yamato-790729 and to develop better CL barometer for wider applications. Furthermore, this study has sought to assign their emission centers and clarify variations on CL signal intensity by shock pressure and chemical composition. For comparison with natural ones, we used several samples of experimentally shock-recovered plagioclase as well as synthetic K-lingunite prepared at static pressures as references.

EXPERIMENTAL METHODS AND MATERIALS

We used two thin sections of L6 chondrites of Tenham from the Department of Geology and Paleontology, National Museum of Nature and Science, Japan and Yamato-790729 from the National Institute of Polar Research, Japan. Under optical and electron microscopic observations, Tenham consists of olivine,

orthoenstatite, diopside, and plagioclase, with accessory minerals such as metallic Fe-Ni and troilite (Tomioka et al. 2016). It shows a network of shock veins in which rounded fragments of host minerals, and several high-pressure minerals of wadsleyite, ringwoodite, majorite, majorite-pyroxene, akimotoite, bridgmanite, and Na-lingunite are observed (Tomioka et al. 2000; Gillet et al. 2007; Tomioka and Miyahara 2017). Yamato-790729 contains large amounts of olivine, low-Ca pyroxene, plagioclase, metallic Fe-Ni, and iron-sulfide with minor phosphate and chromite (Kato et al. 2017), and shows a shock vein and remnants of chondritic textures. Ringwoodite, majorite, akimotoite, and Na-lingunite are present in the shock vein, indicating impact events (Kato et al. 2017; Tomioka and Miyahara 2017).

In the present study, CL microscopic and spectroscopic analyses were conducted for plagioclase, maskelynite, and lingunite in two thin sections. Here, the term “maskelynite” denotes high-density plagioclase glass formed by natural impact events that meteorites and impactites experienced. Their phase and chemical compositions of these feldspar minerals were determined using Raman spectroscopy and by wavelength-dispersive X-ray spectroscopy (WDS) using an electron probe microanalyzer (EPMA), as described in the following section. Results from the chemical analysis and the microprobe settings were reported in Tomioka et al. (2000) for Tenham and Kato et al. (2017) for Yamato-790729. Distribution of these feldspar minerals were analyzed by CL images, as will be described in the following section.

Shock recovery experiments were carried out to prepare reference samples at known shock pressures. We used single crystals of Na-rich plagioclase ($\text{Or}_2\text{Ab}_{98}$) from Marumori, Japan, Ca-Na plagioclase ($\text{Or}_2\text{Ab}_{51}\text{An}_{47}$) from Iwo Jima, Tokyo, Japan, and Ca-rich plagioclase ($\text{Ab}_{17-23}\text{An}_{77-83}$) coarse grain-bearing troctolite. Each sample was sliced perpendicular to the *c*-axis and doubly polished into a flat disk (8 mm diameter, 1 mm thickness) and enclosed in SUS304 stainless steel containers (30 mm diameter \times 30 mm length). A propellant gun with a 30 mm bore at the National Institute for Materials Science, Japan was employed to accelerate a projectile with a metal flyer (8 mm thick Al alloy or 3 mm thick SUS304) to a required velocity. The shock pressure produced in sample was assumed to reach an equilibrium, judging from the thickness ratio of flyer to the samples, with that of the container due to shock wave reverberation within sample, and was determined using the impedance match method from the measured velocity of projectile and the known Hugoniot. Details on shock experiments have been described by Sekine (1997), Yamaguchi and Sekine (2000), and Kayama et al. (2012). We performed

in total six recovery experiments on Na-rich plagioclase at peak shock pressures of 11.1, 21.0, 33.0, and 41.2 GPa and both Ca-Na and Ca-rich plagioclase at 31.7 and 29.7 GPa, respectively. The recovered samples by shock experiments above 33.0 GPa for Na-rich plagioclase, at 31.7 GPa for Ca-Na plagioclase, and at 29.7 GPa for Ca-rich plagioclase were transformed to diaplectic feldspar glasses. Here, the term “diaplectic feldspar glass” is a name that is used to describe high-density feldspar glass formed through solid-state reaction and recovered from shock experiments. K-lingunite was synthesized from adularia at ~ 15 GPa and ~ 1200 °C for 1 h using a multianvil press at the Institute for Study of the Earth’s Interior, Okayama University, and confirmed by X-ray diffraction analysis and Raman spectroscopy.

Color CL images were captured at 15 kV accelerating voltage and 0.5 mA beam current with 30 s exposure using a cold-cathode microscope (Luminoscope) consisting of an optical microscope, an electron gun, and a cooled charge-coupled device (CCD) camera. A scanning electron microscopy-cathodoluminescence (SEM-CL) instrument (a JEOL: JSM-5410 SEM combined with a grating monochromator of Oxford: Mono CL2 and MiniCL imaging system of Gatan) was used to obtain CL spectra and high-resolution panchromatic CL images. All CL spectra in the wavelength range from 300 to 800 nm in 1 nm steps were corrected for the total instrumental response, which was determined using a calibrated standard lamp (Eppley Laboratory: Quartz Halogen Lamp) by the procedure reported in Stevens-Kalceff (2009) and Kayama et al. (2010, 2012). The operating conditions were set at 15 kV accelerating voltage and 2.0 nA beam current in scanning mode with a $44 \mu\text{m} \times 37 \mu\text{m}$ scanning area for the synthetic and experimentally shock-recovered samples and $1 \mu\text{m}$ spot size in diameter for meteoritic samples. Following previous studies (Stevens-Kalceff 2009; Kayama et al. 2010, 2012), the corrected CL spectra of the feldspar samples in energy units were nonlinearly deconvolved into the Gaussian components corresponding to each emission center using the peak-fitting software (Peak Analyzer) implemented in OriginPro 8J SR2. Details of the equipment construction and analytical procedures are in Kayama et al. (2010).

Raman spectroscopy on the Tenham and Yamato-790729 samples was used to identify phases with a laser micro-Raman spectrometer (Thermo Electron; Nicolet: Omega XR) at Okayama University of Science. The laser power (Nd: YAG, 532 nm excitation line) was fixed at 10 mW on the sample with a spot size of ca. $2 \mu\text{m}$. Spectra were collected in 10 accumulations of 15 s exposure. All spectral data were calibrated by the position of the O-Si-O bending vibration of high

optical grade standard quartz before and after each measurement, ensuring reproducibility within $\sim 1 \text{ cm}^{-1}$.

RESULTS

Feldspars in Tenham and Yamato-790729 chondrites have been identified in previous electron microscopy studies (Tomioka et al. 2000; Kato et al. 2017) and by micro-Raman spectroscopy in the present study. Shock veins with a few hundred micrometer width occur within these meteorites, having a total distance of $\sim 10 \text{ mm}$ for Tenham and $\sim 60 \text{ mm}$ for Yamato-790729. In Yamato-790729, the shock vein contains Na-lingunite as flowed micrograins with $\sim 100 \mu\text{m}$ diameters. Transmission electron microscope (TEM) of the Tenham chondrite revealed monomineralic nanocrystalline lingunite with several tens of nanometer-sized aggregates inside the shock vein (Tomioka et al. 2000). Most of maskelynite grains ($\sim 100 \mu\text{m}$) in Tenham and Yamato-790729 chondrites are in contact with or lie close to the shock veins. Plagioclase crystals without maskelynite also occur far from the shock veins in the chondrites.

CL Microscopy

Figure 1 shows color CL images of lingunite, maskelynite, and plagioclase in the Tenham meteorite as bright blue, dull blue, and aqua blue emissions, respectively. Lingunite micrograins in the shock veins display heterogeneous distribution of the emission intensity in the high-resolution panchromatic CL images, which consist of dull emitting stripes and patches with bright luminescent matrix (Figs. 2a and 2b). The prolonged electron-irradiated areas in lingunite during EPMA and CL measurements show appreciably dark CL circular textures on the bright luminescent background. The high-resolution CL images of lingunite micrograins in Yamato-790729 showed dark luminescent circulars as the prolonged electron-irradiated spots with $\sim 5 \mu\text{m}$ diameters (Figs. 2c and 2d). Maskelynite portions near the shock veins in Tenham and Yamato-790729 (Fig. 3) displayed similar dark circles (~ 1 to $\sim 5 \mu\text{m}$ diameters) and rectangles ($\sim 12 \times 9 \mu\text{m}^2$) on homogeneously dull luminescent background. Feldspar grains (a few tens to hundreds of micrometers size) in Yamato-790729 change gradually the color from bright luminescence of vein-shaped maskelynite to dull emitting of matrix plagioclase as the distance increases from the shock vein (Kato et al. 2017). However, plagioclase crystals far from the shock veins in Tenham and Yamato-790729 have homogeneous distribution in the CL intensity (Fig. 4).

CL Spectroscopy

Figure 5 illustrates CL spectra of lingunite in Tenham and Yamato-790729 and synthetic lingunite. Two intense emission bands at ~ 330 and $\sim 380 \text{ nm}$ in the UV–blue region and a weak broad band centered at $\sim 590 \text{ nm}$ in the yellow region were observed from lingunite micrograins in Tenham. Yamato-790729 lingunite micrograins showed similarly intense bands (~ 330 and $\sim 360 \text{ nm}$) and a weak one ($\sim 590 \text{ nm}$) with an additional band centered at $< 300 \text{ nm}$. CL spectra of maskelynite in both Tenham and Yamato-790729 showed UV and blue emissions at ~ 330 and $\sim 380 \text{ nm}$ (Fig. 6), respectively, of which the peak wavelengths are quite similar to those of the lingunite, especially in Tenham (Fig. 5). A weak emission band at $< 300 \text{ nm}$ occurs in CL spectra of maskelynite in these meteorites. Plagioclase crystals in these meteorites have a broad emission band at $\sim 420 \text{ nm}$ (Fig. 6), which have been known to be assigned to Ti^{4+} or Al-O^- -Al/Ti center (Götze et al. 2000, 2013; Götze 2012). Their peak wavelengths and band shapes differ significantly from those detected in lingunite and maskelynite (Figs. 5 and 6). The blue emission intensity of the plagioclase is comparable to UV–blue intensity of the maskelynite, but approximately 10 times lower than that of the lingunite (Figs. 5 and 6).

Synthetic K-lingunite has similar UV–blue CL emission bands (< 300 , ~ 330 , and 360 – 380 nm) (Fig. 5). Its CL spectral patterns are almost the same as those of the lingunite in Yamato-790729 and are similar to those of the lingunite in Tenham as well as the meteoritic maskelynite (Figs. 5 and 6). Additionally, several weak narrow peaks at ~ 550 , ~ 590 , ~ 660 , ~ 720 , ~ 750 , and $\sim 770 \text{ nm}$ are seen in CL spectra of synthetic K-lingunite (Fig. 5). These UV–blue emission bands as well as yellow–IR peaks have significantly higher CL intensities than the corresponding signals of the meteoritic lingunite and maskelynite.

Figure 7a shows CL spectra of several emission bands (320 , 360 , 570 , and 750 nm) for unshocked and experimentally shocked Na-rich plagioclase at 11.1 and 21.0 GPa . They are assigned to Ce^{3+} , Eu^{2+} , Mn^{2+} , and Fe^{3+} impurity centers (Götze et al. 2000; Kayama et al. 2009) (Table 1). Intensities of these UV to IR emission bands appear to decrease with increasing peak shock pressure. Characteristic UV–blue emission bands (< 300 , ~ 330 , and 380 nm) were detectable in diaplectic Na-rich plagioclase glasses recovered at 33.0 and 41.2 GPa and there appears to be a positive correlation between emission intensity and shock pressure (Fig. 7b). Similar UV–blue emission bands are also recognized in CL spectra of diaplectic glasses of Ca-Na and Ca-rich plagioclase recovered at 31.7 and 29.7 GPa , respectively

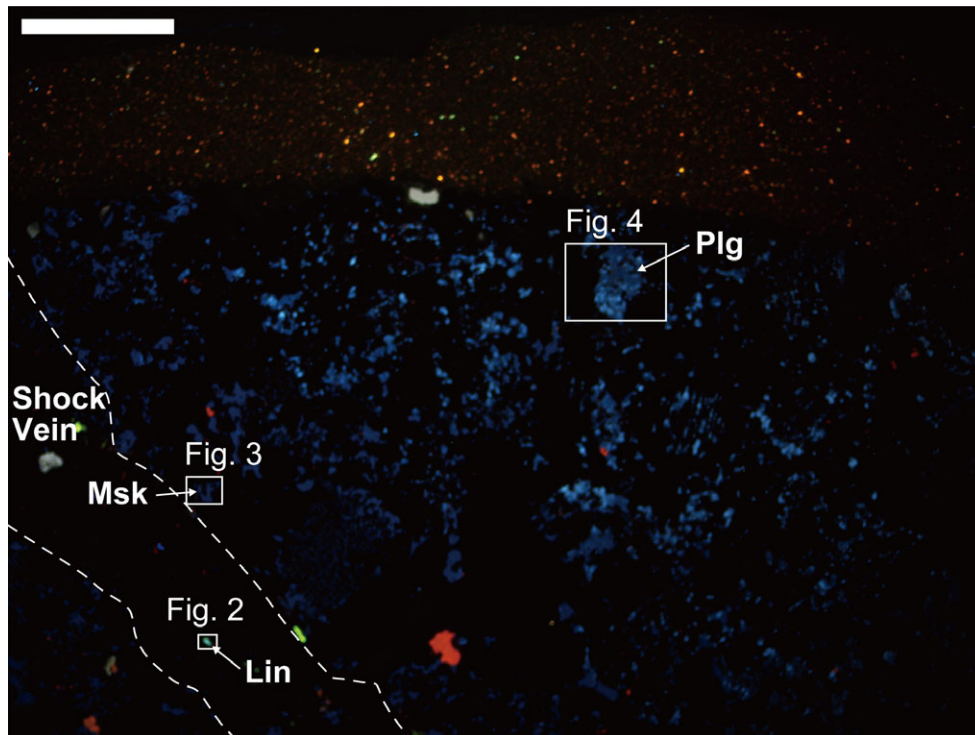


Fig. 1. Color CL images obtained in a thin section from Tenham meteorite. Bright blue luminescent lingunite (Lin), dull blue maskelynite (Msk), and aqua blue plagioclase (Plg) are observed. White-boxed areas are extended in Figs. 2, 3, and 4, respectively. The white scale bar is 1 mm.

(Fig. 8). These recovered diaplectic glasses as well as the meteoritic maskelynite, however, show much lower UV–blue CL intensities than synthetic lingunite and meteoritic lingunite (Figs. 5–7).

DISCUSSION

Maskelynite and Diaplectic Glass

CL spectra characterized by the emission bands at <300 , ~ 330 , and ~ 380 nm are found in only maskelynite (a high-density feldspar glass formed by natural impact event on meteorites) and diaplectic feldspar glasses (a high-density feldspar glass derived through a solid-state reaction and recovered from shock experiment) with the Na–Ca compositions (Figs. 7 and 8), but not in plagioclase in meteorites and feldspars recovered below 21.0 GPa (Figs. 6 and 7). CL spectral patterns similar to those of maskelynite and diaplectic Na–Ca feldspar glasses have also been recognized in alkali feldspar glasses in Martian meteorites and impactites as well as diaplectic alkali feldspar glasses recovered from shock experiments (Kayama et al. 2012). However, it has not been reported in the previous CL studies of feldspars in terrestrial and extraterrestrial rocks, as summarized in Table 1 (Götze et al. 2000, 2013; Götze 2012). CL

spectroscopy of the shock-recovered diaplectic Na-rich plagioclase glass demonstrates that these UV–blue emission intensities tend to increase with increasing shock pressure (Fig. 7), likely the case of previously studied K-feldspar (Kayama et al. 2012). The observations suggest that the UV–blue emission bands are characteristic signals of maskelynite and diaplectic feldspar glasses and that they are closely related to shock metamorphism.

According to the deconvolution method suggested by the previous studies (Stevens-Kalceff 2009; Kayama et al. 2010, 2012), the UV–blue emission bands of the maskelynite and diaplectic feldspar glasses can be separated into three components at 3.88, 3.26, and 2.95 eV by Gaussian fitting (Fig. 9). The number, peak position, and full width half maximum (FWHM) of these Gaussian components can be determined for 20 spectral data of the present samples by the procedure and reference values reported in Kayama et al. (2010, 2012). The former two components have also been reported previously in the deconvolved CL spectra of naturally and shock-recovered alkali feldspar glasses, while the latter component has been in both shock-induced structural and vitreous alkali feldspars (Kayama et al. 2012). Since the components at 3.88, 3.26, and 2.95 eV commonly occur in shock-recovered

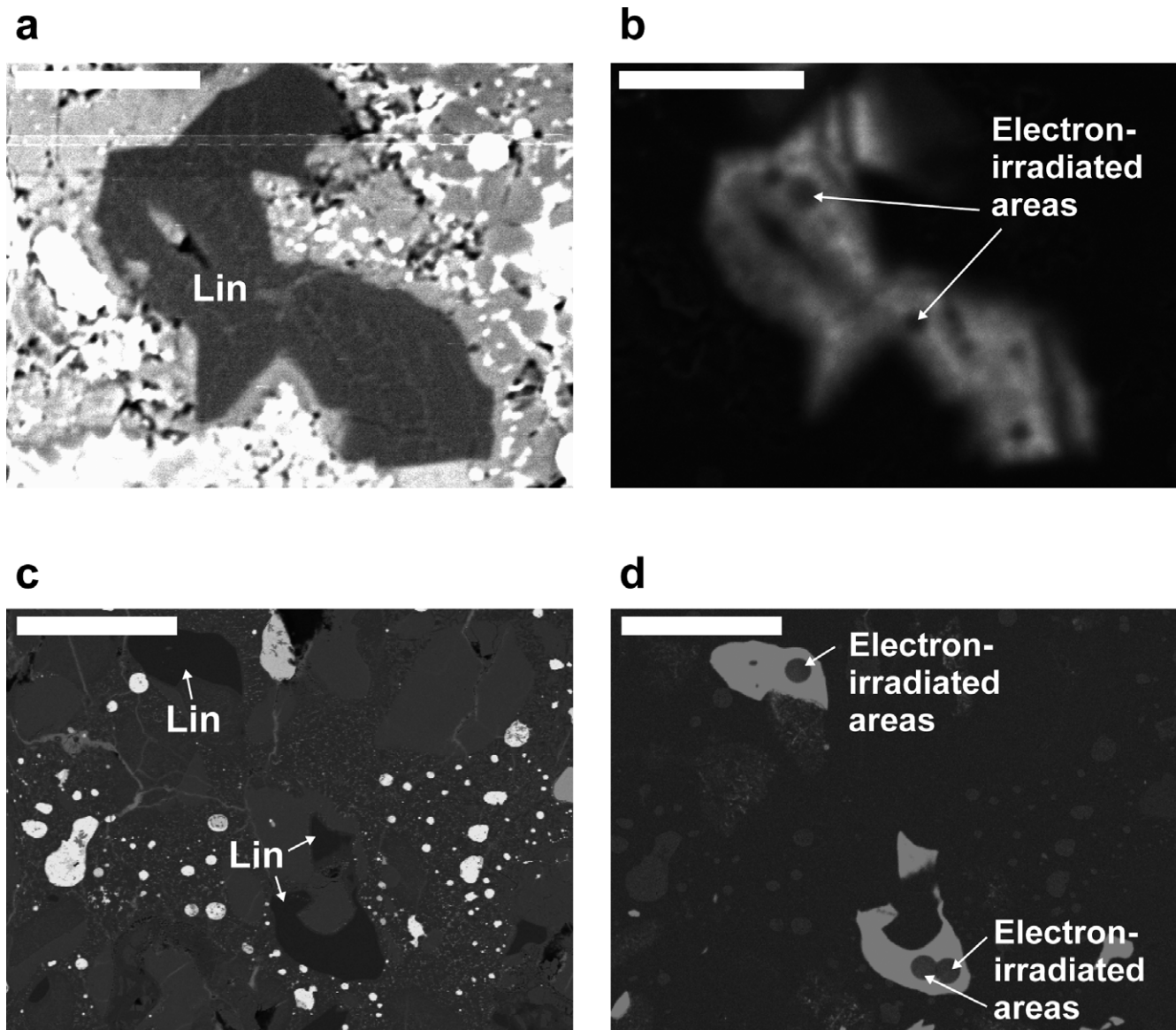


Fig. 2. Backscattered electron (BSE) and high-resolution panchromatic CL images of lingunite (Lin) in Tenham (a, b) and Yamato-790729 (c, d). The electron irradiation areas are indicated by circular textures with dark luminescence. Scale bars (white lines) are 20 μm in (a) and (b), and 100 μm in (c) and (d), respectively.

K-, Na-, and Ca-feldspars and its diaplectic glasses, they can be assigned to the same kinds of lattice defects or impurities that act as luminescence centers. Impurity centers cause CL of unshocked feldspars, but they will not play a role in activator of heavily shocked feldspar and diaplectic glasses because of shock-induced destructions of linkages between the impurities and the ligand atoms (Kayama et al. 2009, 2012). Similarly, in the samples from present shock experiments, pronounced UV to IR emission bands assigned to Ce^{3+} , Eu^{2+} , Mn^{2+} , and Fe^{3+} appear only in CL of the unshocked feldspar, and at high shock pressures, they reduced the CL intensities and disappeared finally in

those of diaplectic glasses (Fig. 7). Therefore, the components at 3.88, 3.26, and 2.95 eV are attributed to the lattice defects in K-, Na-, and Ca-feldspars, because the Al and Si framework structures are changed by shock pressure, as reported previously by Kayama et al. (2012).

The structure of maskelynite and diaplectic feldspar glasses is composed of both octahedra and tetrahedra of Al and Si atoms, and their structural changes by pressure occur depending on the compositional ratio of Al/Si because the Al-O bonds are weaker than the Si-O bonds (Fritz et al. 2005, 2011). The components at 3.26 and 3.88 eV, detected only in diaplectic feldspar glasses,

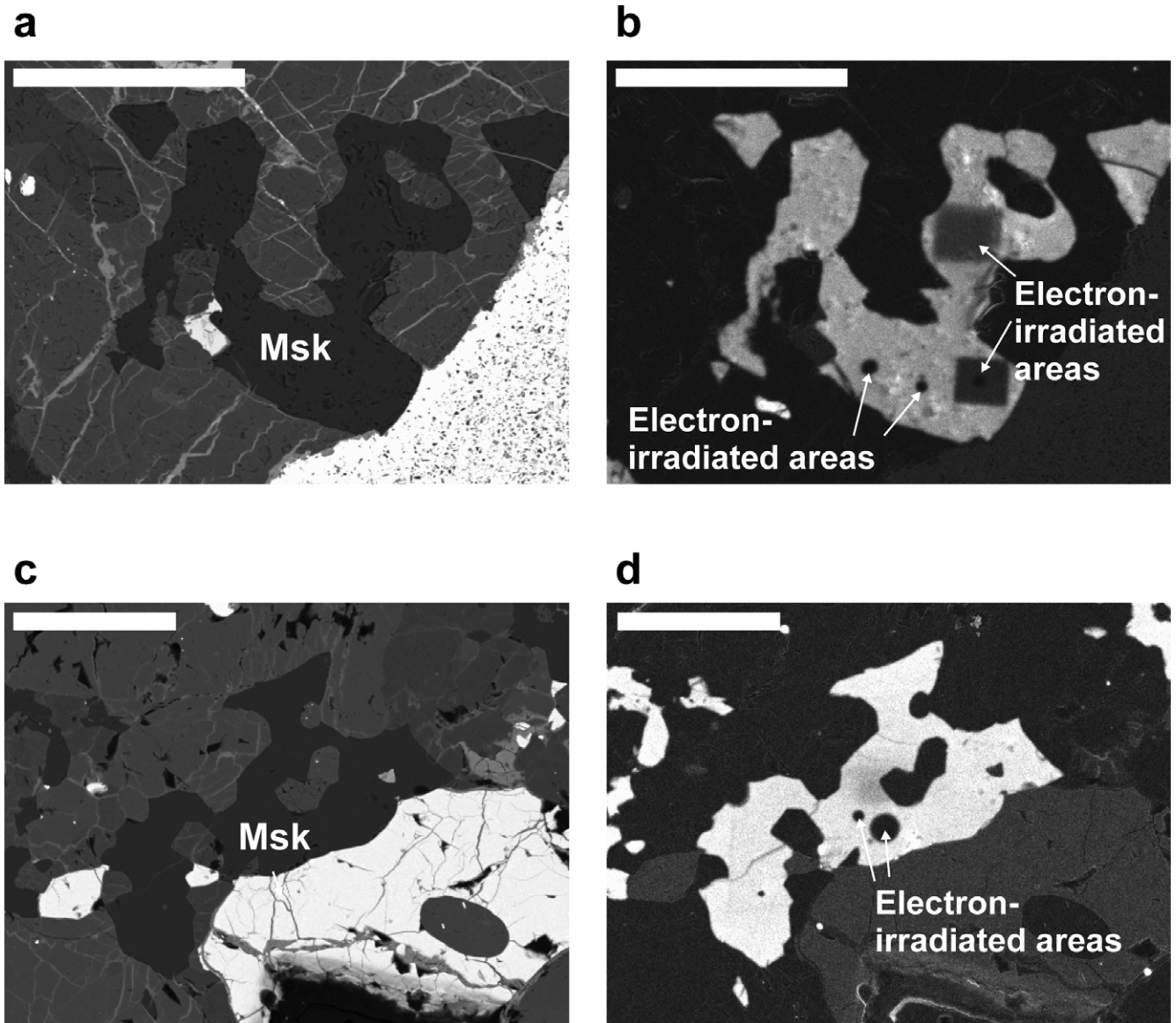


Fig. 3. BSE and high-resolution CL images of maskelynite (Msk) in Tenham (a, b) and Yamato-790729 (c, d). The electron irradiation areas are indicated by square- or circle-shaped textures with dark luminescence. Scale bars (white lines) are 100 μm .

show positive correlations between emission intensity and shock pressure. It has been known that the gradient of the intensity at 3.26 eV against shock pressure shows no significant change up to a pressure of 40.1 GPa and that the one at 3.88 eV decreases gradually with shock pressure above 31.7 GPa (Kayama et al. 2012). The components at 3.26 and 3.88 eV may have been assigned to pressure-induced defect centers in the Si and Al octahedra, respectively. This can be interpreted by the following model. Most of the Al-O bonds in the structure may be broken by shock pressure above 31.7 GPa, and then the population of the pressure-induced defects in Al octahedra reaches the saturation

level. In contrast, a large amount of the Si-O bonds remain even if the feldspar is subject to a shock pressure of 40.1 GPa, because the intensity at 3.26 eV correlates linearly with shock pressure up to 40.1 GPa (Kayama et al. 2012). Because the emission component at 2.95 eV occurs in both crystal and diaplectic feldspar after natural and experimental shock, it may be assigned to pressure-induced defect in Si and/or Al tetrahedra. For more detailed interpretation, one can refer to Kayama et al. (2009, 2012).

The emission intensity at 2.95 eV for Na-rich plagioclase recovered at 33.0 GPa can be compared at a similar shock pressure with those of K-feldspar at

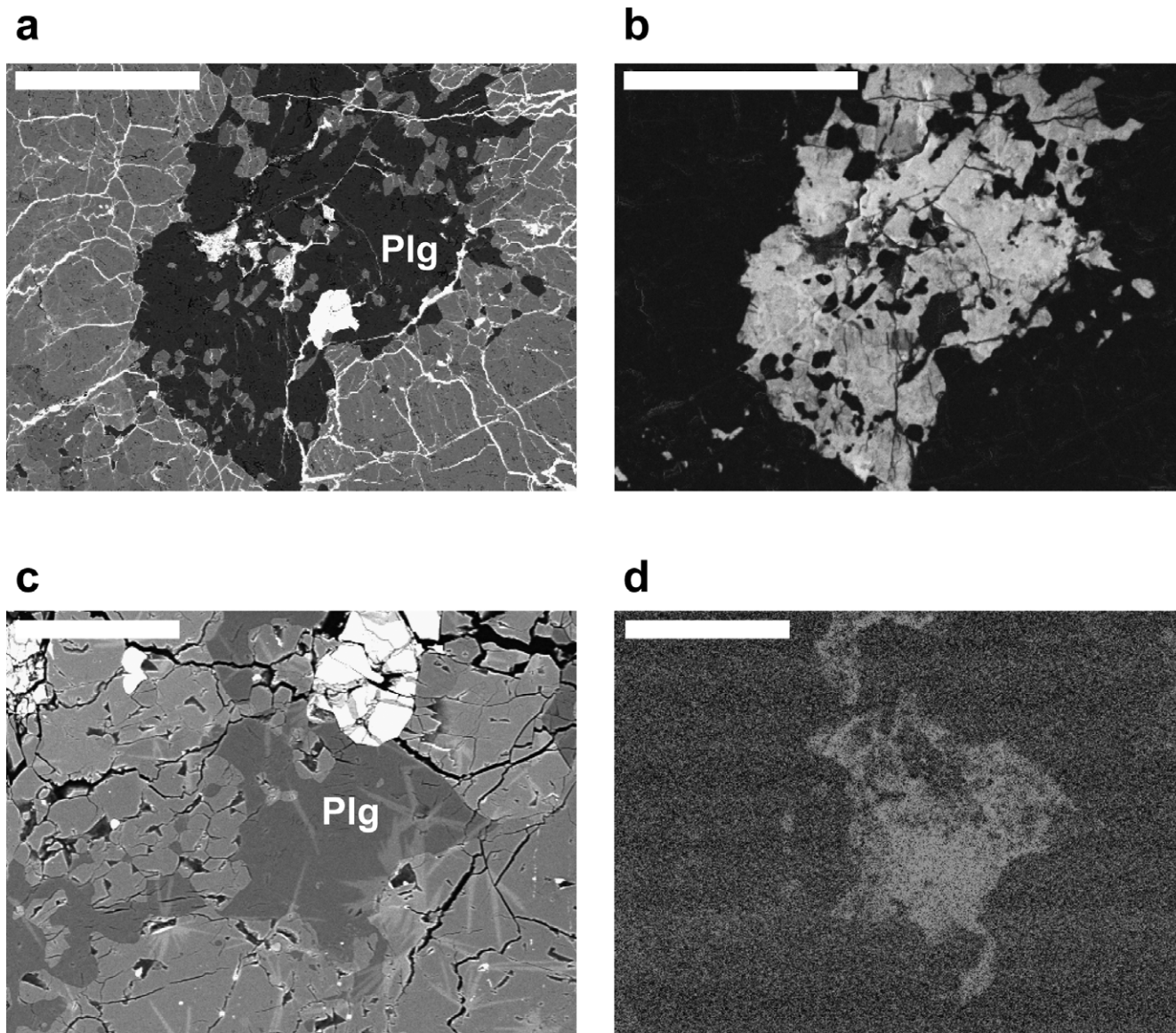


Fig. 4. BSE and high-resolution CL images of crystalline plagioclase (Plg) in Tenham (a, b) and Yamato-790729 (c, d). Scale bars (white lines) are 200 μm in (a) and (b), and 100 μm in (c) and (d), respectively.

31.7 GPa and microcline at 33.0 GPa (Kayama et al. 2012). They are very similar in spite of different chemical compositions. Therefore, a response of the emission intensity at 2.95 eV appears to be controlled mainly by shock pressure as a function of population of the pressure-induced defects and may be little dependent on chemistry. Kayama et al. (2012) have indicated that the emission intensity at 2.95 eV in shocked alkali feldspar may depend on shock pressure but not on the in-shock and postshock temperatures. The emission intensity at 2.95 eV will be used to estimate shock pressures in K-, Na-, and Ca-feldspar-bearing meteorites and impactites once a reliable relationship

between emission intensity at 2.95 eV and shock pressure is acquired using the shock-recovered samples at known pressure.

The emission components at 3.26 and 3.88 eV are detectable in meteoritic maskelynite and diaplectic feldspar glasses (Fig. 9), but not in crystalline feldspars in meteorites and the shock-recovered samples, indicating a close relationship between their CL properties and a vitrification of feldspar due to shock metamorphism. Since new defect centers in the octahedral sites of the feldspar structure are generated by high shock pressures due to the broken Si-O and Al-O bonds, the emission intensities at 3.26 and 3.88 eV

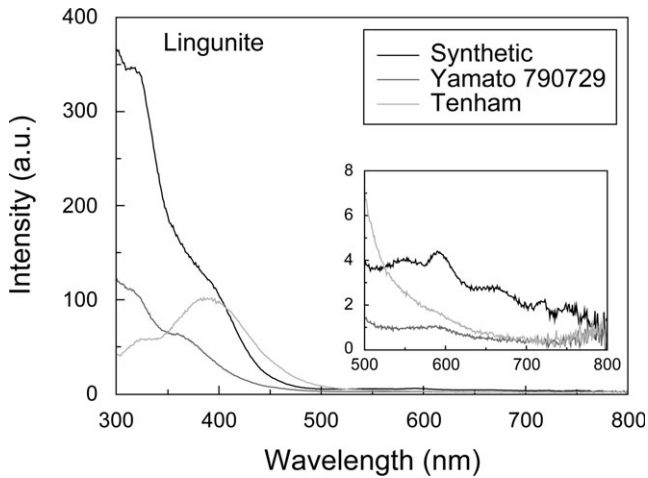


Fig. 5. Comparison of CL spectra between Na-lingunites in Tenham and Yamato-790729 and synthetic K-lingunite.

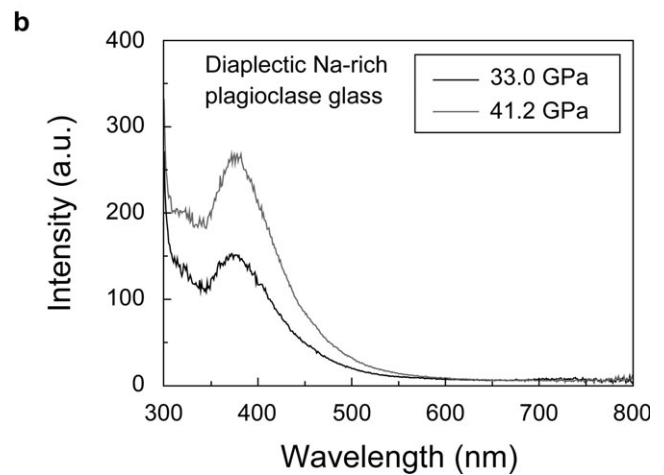
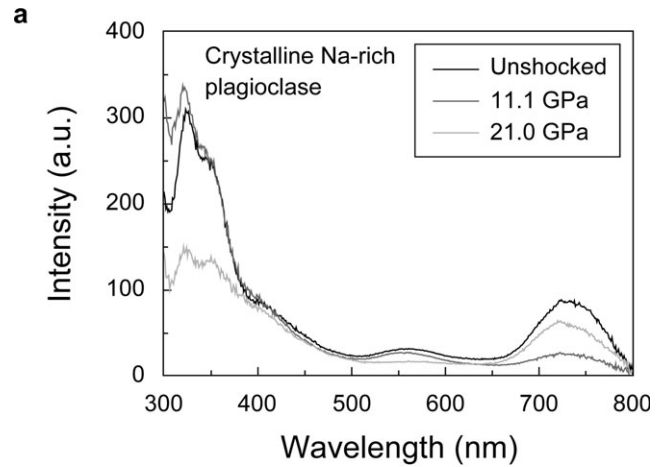


Fig. 7. CL spectra of (a) the initial and experimentally shock-recovered Na-rich plagioclase at 11.1 and 21.0 GPa and (b) the diaplectic glasses of Na-rich plagioclase shock-recovered at 33.0 and 41.2 GPa.

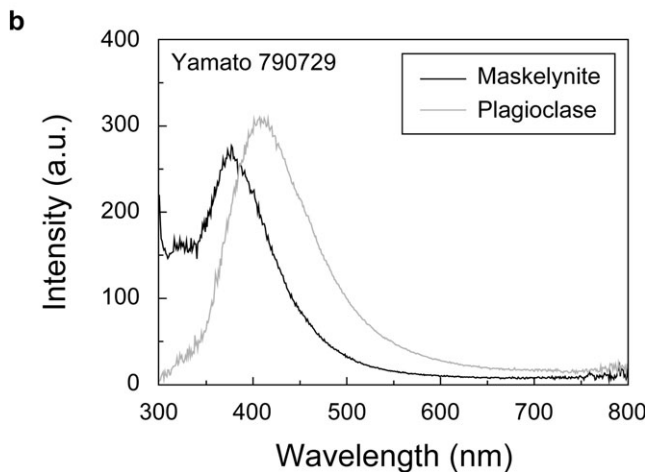
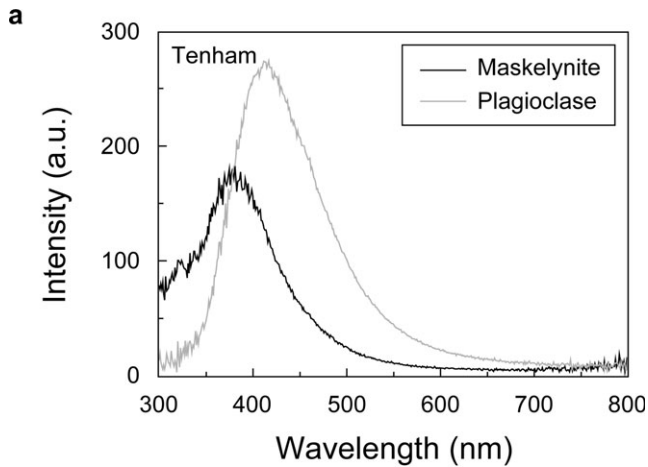


Fig. 6. Comparison of CL spectra between maskelynite and plagioclase in (a) Tenham and (b) Yamato-790729, respectively.

can be described as a function of the defect density above a threshold pressure of transition from feldspar to diaplectic glass and are affected by the Al/Si ratio as their chemical compositions (Ostertag et al. 1986; Fritz et al. 2005, 2011). The emission intensities at 3.26 and 3.88 eV can be applicable to evaluate the shock degree of maskelynitization in meteorites and impactites, based on the experimental results on vitrification of feldspar at known shock pressures.

Lingunite

The UV–blue emission bands at <300, ~330, and 360–380 nm of the Yamato-790729 lingunite and synthetic lingunite (Fig. 5) have been deconvolved into three components at 3.88, 3.45, and 3.26 eV, whereas those in the Tenham lingunite have been separated into the components at 3.88, 3.26, and 2.95 eV (Fig. 9). The

Table 1. Various types of luminescence centers identified here and reported previously.

Wavelength (nm)	Energy (eV)	Type of luminescence centers	Minerals
320		Ce ³⁺ impurity	Plg
~330	3.88	Defect in Al octahedra	Lin, Msk, DG
360–380	3.26	Defect in Si octahedra	Lin, Msk, DG
	3.45	Defect in Si and/or Al octahedra	Lin
	2.95	Defect in Si and/or Al tetrahedra	Shocked feldspars
360		Eu ²⁺ impurity	Plg
420	3.07	Ti ⁴⁺ impurity	Plg
	2.84	Al-O ⁻ -Al/Ti center	Plg
550		Defect in Si and/or Al octahedra	Lin
570		Mn ²⁺ impurity	Plg
590		Defect in Si and/or Al octahedra	Lin
		Defect in Si and/or Al octahedra	Synthetic K-Lin
660		Defect in Si and/or Al octahedra	Synthetic K-Lin
720		Defect in Si and/or Al octahedra	Synthetic K-Lin
750		Defect in Si and/or Al octahedra	Synthetic K-Lin
750		Fe ³⁺ impurity	Plg
770		Defect in Si and/or Al octahedra	Synthetic K-Lin

Lin, Msk, DG, and Plg indicate lingunite, maskelynite, diaplectic glass, and plagioclase, respectively.

component at 2.95 eV may come from maskelynite filling between nanograins of lingunite. Meteoritic maskelynite and the shock-recovered diaplectic feldspar glasses also show the components at 3.88 and 3.26 eV assigned to the pressure-induced defect centers in Al and Si octahedra. It is noteworthy that these CL signals are commonly derived from feldspars with octahedral structure. The lingunite has approximately two or three order higher emission intensities at 3.26 and 3.88 eV than maskelynite and shock-recovered diaplectic glasses. This difference may be responsible for the ratio of Si and Al octahedra to the tetrahedra between lingunite and vitreous feldspar. Structurally, lingunite comprises totally Si and Al octahedra, but maskelynite as well as diaplectic feldspar glass consists of various ratios of frameworked octahedra and tetrahedra depending on the degree of vitrification. In other words, lingunite has more abundant precursors of the pressure-induced defect centers in Si and Al octahedra than maskelynite and diaplectic glass.

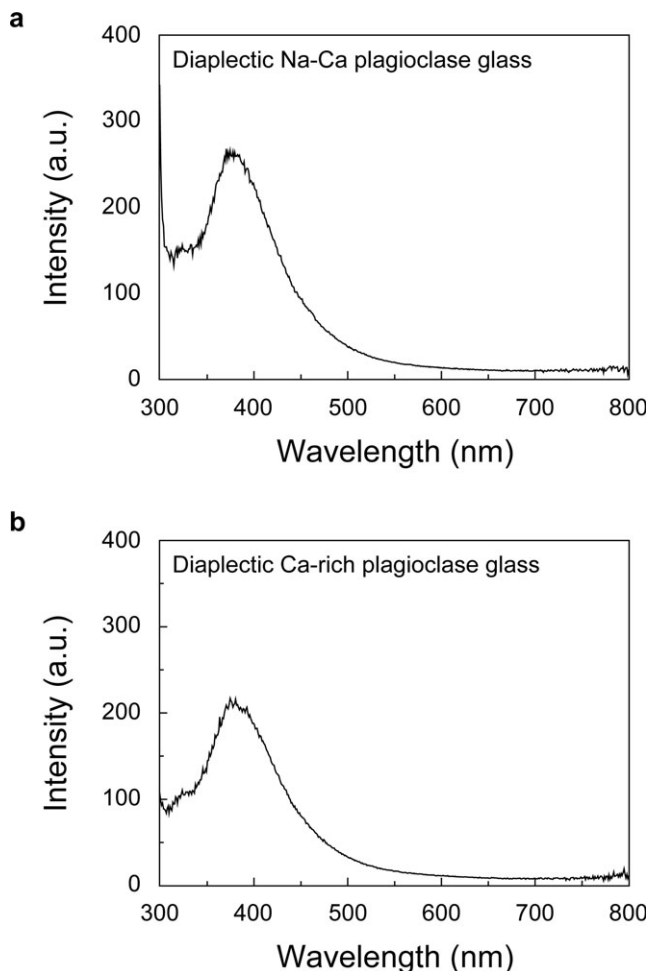


Fig. 8. CL spectra of experimentally shock-recovered products of (a) Ca-Na plagioclase at 31.7 GPa and (b) Ca-rich plagioclase at 29.7 GPa.

Deconvolved CL spectra of the lingunite also contain additional components at 3.45 eV in the UV–blue region (Fig. 9), characteristic yellow–IR emission bands at ~590 nm for all lingunite samples, and at ~550, ~660, ~720, ~750, and ~770 nm for the synthetic sample (Fig. 5). However, no such CL emission component or band has been observed in the maskelynite, shock-recovered diaplectic feldspar glasses, and previously reported feldspar minerals (e.g., Finch and Klein 1999; Götze et al. 2000; Lee et al. 2007; Kayama et al. 2010, 2012). CL signals corresponding to the components at 3.45 eV and bands at ~590 nm commonly appear in K-rich and Na-rich lingunite, in spite of the different chemical composition, and therefore may be attributed to pressure-induced defect centers in the lingunite structure. Such defect centers in lingunite may be produced by shock-induced distortion or dislocation of the Si and Al octahedral structure rather than destruction of the bonds between the cations and

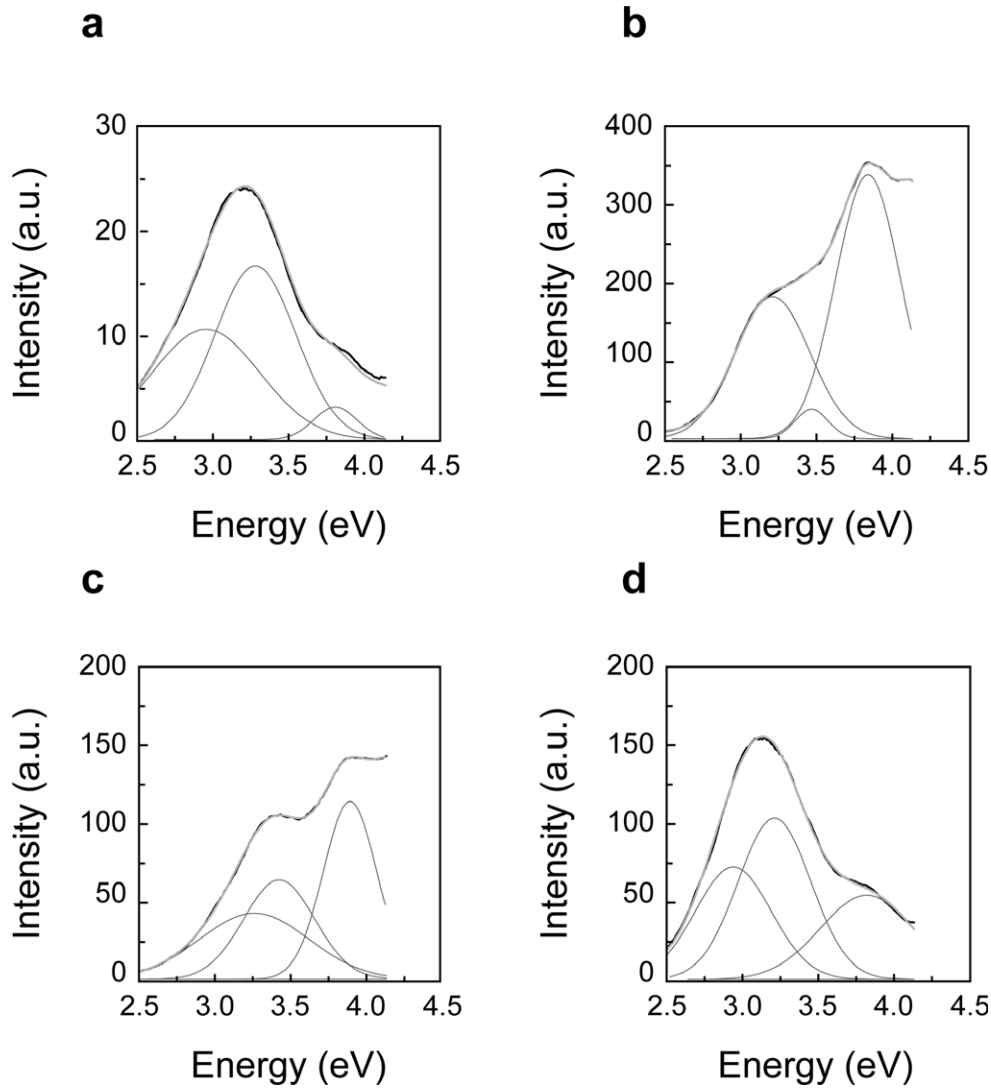


Fig. 9. Deconvolution of CL spectra in energy units obtained from (a) maskelynite in Tenham, (b) synthetic K-lingunite, and Na-lingunite in Yamato-790729 (c) and Tenham (d).

oxygen, because their CL signals are absent in maskelynite and diaplectic feldspar glasses. The pressure-induced defect centers attributed to the components at 3.88, 3.45, and 3.26 eV as well as the bands at ~ 590 nm are likely to change with shock pressure.

CONCLUSIONS

Various types of luminescence centers identified here and reported in previous works are summarized in Table 1, suggesting that CL spectroscopy with high spatial resolution ($\sim 1 \mu\text{m}$) can be applied as an identification method for feldspar polymorphs. The CL properties of maskelynite and lingunite depend on not only the shock pressure but also several other factors

such as shock temperature, strain, and duration, since there is a considerable difference in the presence or absence of emission components, their intensities, and their peak FWHM among feldspars in the meteoritic, shock-recovered, and synthetic samples. Synthetic K-lingunite shows appreciably higher UV-blue intensity than meteoritic lingunite. The emission bands at ~ 550 , ~ 660 , ~ 720 , ~ 750 , and ~ 770 nm were observed in the synthetic samples, but not recognized in the meteoritic grains. It is usually assumed that actual asteroid collisions may retain long shock duration times of 10^{-1} to 10^{-2} s (Ohtani et al. 2004; Xie et al. 2006; Miyahara et al. 2010, 2013), while typical shock experiment lasts for 10^{-5} to 10^{-6} s, and static experiments for 10^2 to 10^3 s. Accordingly, the maskelynitization and phase transition kinetics of feldspar due to shock

metamorphism are of great importance for the estimation of shock pressure that meteorites and impactites experienced. Of course, shock temperature affects CL features of maskelynite (Kayama et al. 2012) and lingunite. Thus, CL analysis of these high-pressure feldspar minerals, especially maskelynite, may be potentially used for a shock barometer for various samples of stony meteorites and samples returned by spacecraft missions, although the further validation of effects on the CL properties such as shock temperature, strain, and duration will be necessary for more precious and reliable improvement.

Acknowledgments—We are deeply indebted to Dr. D. Yamazaki (Institute for Study of the Earth's Interior Okayama University, Japan) for synthesis of K-lingunite using multianvil press and the allocation for this study. We thank Mr. Y. Shibata (Technical center, Hiroshima University, Hiroshima, Japan) for EPMA analysis using JXA-8200 at the Natural Science Center for Basic Research and Development (N-BARD), Hiroshima University. We also appreciate the National Institute of Polar Research (Tokyo, Japan) for kindly allocating the Yamato-790729 sample. Part of this work was supported by JSPS KAKENHI Grant Number 25800294.

Editorial Handling—Dr. Gordon Osinski

REFERENCES

- Boggs S. J. R., Krinsley D. H., Goles G. G., Seyedolali A., and Dypvik H. 2001. Identification of shocked quartz by scanning cathodoluminescence imaging. *Meteoritics & Planetary Science* 36:783–791.
- Chen M. and El Goresy A. 2000. The nature of maskelynite in shocked meteorites: Not diaplectic glass but a glass quenched from shock-induced dense melt at high pressures. *Earth and Planetary Science Letters* 179:489–502.
- Chennaoui Aoudjehane H., Jambon A., Reynard B., and Blanc P. 2005. Silica as a shock index in shergottites: A cathodoluminescence study. *Meteoritics & Planetary Science* 40:967–979.
- El Goresy A., Chen M., Gillet P., and Dubrovinsky L. S. 2000. Shock-induced high-pressure phase transition of labradorite to hollandite “(Na₄₇-Ca₅₁-K₂)” in Zagami and the assemblage hollandite “(Na₈₀-Ca₁₂-K₈)” + Jadeite in L chondrites: Constraints to peak-shock pressures. *Meteoritics & Planetary Science* 37:A51.
- Finch A. and Klein J. 1999. The causes and petrological significance of cathodoluminescence emission from alkali feldspars. *Contributions to Mineralogy and Petrology* 135:234–243.
- Fritz J., Greshake A., and Stöffler D. 2005. Micro-Raman spectroscopy of plagioclase and maskelynite in Martian meteorites: Evidence of progressive shock metamorphism. *Antarctic Meteorite Research* 18:96–116.
- Fritz J., Wünnemann K., Greshake A., Fernandes V. A. S. M., Boettger U., and Hornemann U. 2011. Shock pressure calibration for lunar plagioclase (abstract #1196). 42nd Lunar and Planetary Science Conference. CD-ROM.
- Fritze B., Götze J., and Lange J.-M. 2017. Cathodoluminescence of moldavites. *Meteoritics & Planetary Science* 52:1428–1436.
- Gillet P., Chen M., Dubrovinsky L., and El Goresy A. 2000. Natural NaAlSi₃O₈-hollandite in the shocked Sixiangkou meteorite. *Science* 287:1633–1636.
- Gillet P., El Goresy A., Beck P., and Chen M. 2007. High-pressure mineral assemblages in shocked meteorites and shocked terrestrial rocks: Mechanisms of phase transformations and constraints to pressure and temperature histories. In *Advances in high-pressure mineralogy*, edited by Ohtani E. Boulder, Colorado: The Geological Society of America. pp. 57–82.
- Götze J. 2012. Application of cathodoluminescence microscopy and spectroscopy in geosciences. *Meteoritics & Planetary Science* 18:1270–1284.
- Götze J., Habermann D., Kempe U., Neuser R. D., and Richter D. K. 1999. Cathodoluminescence microscopy and spectroscopy of plagioclase from lunar soil. *American Mineralogist* 84:1027–1032.
- Götze J., Krbetschek M. R., Habermann D., and Wold D. 2000. High-resolution cathodoluminescence of feldspar minerals. In *Cathodoluminescence in geosciences*, edited by Pagel M., Barbin V., Blanc P., and Ohnenstetter D. Berlin: Springer Verlag. pp. 245–270.
- Götze J., Schertl H.-P., Neuser R. D., Kempe U., and Hanchar J. M. 2013. Optical microscope-cathodoluminescence (OM-CL) imaging as a powerful tool to reveal internal textures of minerals. *Mineralogy and Petrology* 107:373–392.
- Hamers M. F. and Drury M. R. 2011. Scanning electron microscope-cathodoluminescence (SEM-CL) imaging of planar deformation features and tectonic deformation lamellae in quartz. *Meteoritics & Planetary Science* 46:1814–1831.
- Hamers M. F., Pennock G. M., Herwegh M., and Drury M. R. 2016. Distinction between amorphous and healed planar deformation features in shocked quartz using composite color scanning electron microscope cathodoluminescence (SEM-CL) imaging. *Meteoritics & Planetary Science* 51:1914–1931.
- Jaret S. J., Woerner W. R., Phillips B. L., Ehm L., Nekvasil H., Wright S. P., and Glotch T. D. 2015. Maskelynite formation via solid-state transformation: Evidence of infrared and X-ray anisotropy. *Journal of Geophysical Research: Planets* 120:E004764.
- Kato Y., Sekine T., Kayama M., Miyahara M., and Yamaguchi A. 2017. High-pressure polymorphs in Yamato-790729 L6 chondrite and their significance for collisional condition. *Meteoritics & Planetary Science* 52:2570–2585.
- Kayama M., Gucsik A., Nishido H., Ninagawa K., and Tsuchiyama A. 2009. Cathodoluminescence and Raman spectroscopic characterization of experimentally shocked plagioclase. *American Institute of Physics Conference Proceedings* 1163:86–95.
- Kayama M., Nakano S., and Nishido H. 2010. Characteristics of emission centers in alkali feldspar: A new approach by using cathodoluminescence spectral deconvolution. *American Mineralogist* 95:1783–1795.

- Kayama M., Nishido H., Sekine T., Nakazato T., Gucsik A., and Kiyotaka K. 2012. Shock barometer using cathodoluminescence of alkali feldspar. *Journal of Geophysical Research* 117. <https://doi.org/10.1029/2011je004025>.
- Kinomura N., Kume S., and Koizumi M. 1975. Stability of $K_2Si_4O_9$ with wadeite type structure. Paper presented at 4th International Conference on High Pressure, International Association for the Advancement of High Pressure Research and Technology, Kyoto, Japan.
- Kubo T., Kimura M., Kato T., Nishi M., Tominaga A., Kikegawa T., and Funakoshi K. 2010. Plagioclase breakdown as an indicator for shock conditions of meteorites. *Nature Geoscience* 3:41–45.
- Lambert P. 1981. Reflectivity applied to peak pressure estimates in silicates of shocked rocks. *Journal of Geophysical Research* 86:6187–6204.
- Lee M. R., Parson I., Edwards P. R., and Martin R. W. 2007. Identification of cathodoluminescence activators in zoned alkali feldspars by hyperspectral imaging and electron-probe microanalysis. *American Mineralogist* 92:243–253.
- Liu X. 2006. Phase relations in the system $KAlSi_3O_8$ - $NaAlSi_3O_8$ at high pressure-high temperature conditions and their implication for the petrogenesis of lingunite. *Earth and Planetary Science Letters* 246:317–325.
- Marfunin A. S. 1979. *Spectroscopy, luminescence and radiation centers in minerals*. Berlin: Springer Verlag. 352 p.
- Marshall D. J. 1988. *Cathodoluminescence of geological materials*. Boston, Massachusetts: Hyman.
- Miyahara M., Ohtani E., Kimura M., El Goresy A., Ozawa S., Nagase T., Nishijima M., and Hiraga K. 2010. Coherent and subsequent incoherent ringwoodite growth in olivine of shocked L6 chondrites. *Earth and Planetary Science Letters* 295:321–327.
- Miyahara M., Kaneko S., Ohtani E., Sakai T., Nagase T., Kayama M., Nishido H., and Hirao N. 2013. Discovery of seifertite in a shocked lunar meteorite. *Nature Communications* 4:1737.
- Mori H. 1990. Hollandite-type $NaAlSi_3O_8$ in shocked meteorites. Paper presented at the 31st High Pressure Conference of the Japan Society of High Pressure Science and Technology, Osaka, Japan, 134–135.
- Ohtani E., Kimura Y., Kimura M., Takata T., Kondo T., and Kubo T. 2004. Formation of high-pressure minerals in shocked L6 chondrite Yamato 791384: Constraints on shock conditions and parent body size. *Earth and Planetary Science Letters* 227:505–515.
- Ostertag R., Stöffler D., Bischoff A., Palme H., Schultz L., Spettel B., Weber H., Weckwerth G., and Wanke H. 1986. Lunar meteorite Yamato-791197: Petrography, shock history and chemical composition. *Memoirs of National Institute of Polar Research Special Issue* 41:17–44.
- Owen M. R. and Anders M. H. 1980. Evidence from cathodoluminescence for non-volcanic origin of shocked quartz at the Cretaceous/Tertiary boundary. *Nature* 334:145–147.
- Pittarello L., Roszjar J., Mader D., Debaille V., Claeys P., and Koeberl C. 2015. Cathodoluminescence as a tool to discriminate impact melt, shocked and unshocked volcanics: A case study of samples from the El'gygytgyn impact structure. *Meteoritics & Planetary Science* 50:1954–1969.
- Ringwood A. E., Reid A. F., and Wadsley A. D. 1967. High-pressure $KAlSi_3O_8$, an aluminosilicate with sixfold coordination. *Acta Crystallographica*. 23:1093–1095.
- Sekine T. 1997. Shock wave chemical synthesis. *European Journal of Solid State and Inorganic Chemistry* 34: 823–833.
- Supple R. F. and Spencer A. B. 1970. Cathodoluminescence properties of lunar rocks. *Science* 167:677–679.
- Stevens-Kalceff M. A. 2009. Cathodoluminescence microcharacterization of point defects in α -quartz. *Mineralogical Magazine* 73:585–605.
- Stöffler D., Ostertag R., Jammes C., Pfannschmidt G., Sen Gupta P. R., Simon S. B., Papike J. J., and Beauchamp R. H. 1986. Shock metamorphism and petrography of the Shergotty achondrite. *Geochimica et Cosmochimica Acta* 50:889–903.
- Stöffler D., Keil K., and Scott E. R. D. 1991. Shock metamorphism of ordinary chondrites. *Geochimica et Cosmochimica Acta* 55:3845–3867.
- Sueda Y., Irifune T., Nishiyama N., Rapp R. P., Ferroir T., Onozawa T., Yagi T., Miyajima N., Merkel S., and Funakoshi K. 2004. A new unquenchable high-pressure of $KAlSi_3O_8$ under lower mantle conditions. *Geophysical Research Letters* 31:L23612.
- Tomioka N. and Miyahara M. 2017. High-pressure minerals in shocked meteorites. *Meteoritics & Planetary Science* 52:2017–2039.
- Tomioka N., Mori H., and Fujino K. 2000. Shock-induced transition of $NaAlSi_3O_8$ feldspar into a hollandite structure in a L6 chondrite. *Geophysical Research Letters* 27:3997–4000.
- Tomioka N., Miyahara M., and Ito M. 2016. Discovery of natural $MgSiO_3$ tetragonal garnet in a shocked chondritic meteorite. *Science Advances* 2. <https://doi.org/10.1126/sciadv.1501725>.
- Tutti T., Dubrovinsky L. S., Saxena S. K., and Carlson S. 2001. Stability of $KAlSi_3O_8$ hollandite type structure in the Earth's lower mantle conditions. *Geophysical Research Letters* 28:2735–2738.
- Urakawa S., Kondo T., Igawa N., Shimomura O., and Ohno H. 1994. Synchrotron radiation study on the high-pressure and high-temperature phase relations of $KAlSi_3O_8$. *Physics and Chemistry of Minerals* 21:387–391.
- Xie Z., Sharp T. G., and DeCarli P. S. 2006. High-pressure phases in a shock-induced melt vein of the Tenham L6 chondrite: Constraints on shock pressure and duration. *Geochimica et Cosmochimica Acta* 70:504–515.
- Yacobi B. G. and Holt D. B. 1990. *Cathodoluminescence. Microscopy of inorganic solids*. New York: Plenum Press.
- Yagi T., Suzuki T., and Akaogi M. 1994. High pressure transitions in the system $KAlSi_3O_8$ - $NaAlSi_3O_8$. *Physics and Chemistry of Minerals* 21:12–17.
- Yamaguchi A. and Sekine T. 2000. Monomineralic mobilization of plagioclase by shock: An experimental study. *Earth and Planetary Science Letters* 175:289–296.
-